



OPEN Brown adipose tissue transplantation ameliorates hindlimb ischemic damage in diabetic mice

Ting Lu¹, Amin Liu¹, Chunchun Li¹, Yi Li¹, Bin Yang², Qian Liu²✉ & Hua Jiang³✉

Peripheral arterial disease (PAD) is a common complication associated with diabetes, which can lead to foot ischemia. The condition is often accompanied by infection and necrosis, ultimately leading to diabetic foot ulcers and the risk of amputation. Brown adipose tissue (BAT) and its secreted cytokines play an essential role in the regulation of glucose homeostasis, the modulation of inflammatory responses, and vascular endothelial cell proliferation. The transplantation of BAT into ischemic regions may offer therapeutic benefits in alleviating the symptoms associated with PAD. A diabetic mouse model was established via intraperitoneal administration of streptozocin. Subsequently, a diabetic lower limb ulcer model was constructed by transection of the femoral artery and ligation of the femoral vein. BAT harvested from the subscapular region of the mouse was employed as an adipose graft. The research utilized Laser Doppler monitoring, Western blot analysis, hematoxylin-eosin (HE) staining, immunofluorescence staining, and enzyme-linked immunosorbent assay (ELISA) to evaluate blood flow recovery in ischemic regions, histopathological changes, angiogenesis and tissue remodeling, inflammatory responses, and M1/M2 macrophage polarization. BAT transplantation significantly enhanced blood flow recovery in ischemic regions of diabetic lower limb ulcer mice while concurrently reducing necrotic tissue. Pathological analyses demonstrate that BAT transplantation mitigates ischemic tissue damage, stimulates angiogenesis, and supports tissue remodeling. Furthermore, the Western blotting, immunofluorescence, and ELISA results revealed that BAT transplantation significantly reduces inflammatory levels in ischemic tissues, increases the expression of angiogenic factors, and promotes the polarization of macrophages from the M1 to the M2 phenotype. The research has demonstrated that BAT transplantation can mitigate ischemic injury in diabetic lower limb ulcer mice, attenuate inflammatory responses, and facilitate the restoration of blood flow. These effects may be linked to alterations in macrophage polarization.

Keywords Peripheral arterial disease, Diabetic lower limb ulcer mouse model, Brown adipose tissue, Transplantation, Inflammation, Macrophage.

Diabetes is a prevalent disease that seriously threatens human health. Peripheral vascular disease (PVD), a common complication of diabetes, affects major blood vessels in the heart, brain, limbs, and other organs, thereby significantly impacting the health of individuals with diabetes worldwide. Peripheral arterial disease (PAD) affects approximately 20% of individuals with diabetes and is regarded as the most severe and detrimental form of PVD¹. The condition is characterized by stenosis and occlusion of the lower limb arteries. In patients with PAD, poor peripheral circulation frequently leads to ischemic lesions, compounded by infection and necrosis, ultimately resulting in diabetic foot. Such patients might require amputation in as much as 22% of cases². However, the treatment of PAD poses significant challenges, as no particularly effective drugs or treatment approaches have been found so far³. Currently, the treatment of PDA primarily focuses on regulating glucose and lipid metabolism, alongside the application of vasodilators, anticoagulants, antiplatelet agents, and

¹Center for Basic and Translational Research, The Second Affiliated Hospital Zhejiang University School of Medicine, Hangzhou 310009, Zhejiang, PR China. ²School of Pharmaceutical Sciences, Zhejiang Chinese Medical University, Hangzhou 311402, Zhejiang, PR China. ³Department of Otolaryngology, The Second Affiliated Hospital Zhejiang University School of Medicine, Hangzhou 310009, Zhejiang, PR China. ✉email: liuqian@zcmu.edu.cn; zjrjh@zju.edu.cn

neuroprotective strategies. In many diabetic foot patients who develop gangrene, amputation often emerges as the only viable option.

Adipose tissue is abundant in the human body and serves as the principal organ for energy storage. Recent studies have demonstrated that adipose tissue plays a crucial role in the internal microenvironment, such as inflammation and tumor⁴. In addition to energy storage, adipose tissue exerts diverse effects across various physiological and pathological conditions due to its considerable plasticity. Human adipose tissue is categorized into white adipose tissue (WAT) and brown adipose tissue (BAT). WAT primarily functions as energy storage, while BAT regulates energy expenditure and rapid heat generation. Research has shown that BAT contributes to maintaining systemic glucose homeostasis by alleviating inflammation in adipose tissue⁵. Liu et al.^{6,7} demonstrated that the transplantation of BAT can significantly improve the metabolic condition of diabetic and obese murine models. Furthermore, it can reduce blood glucose levels and insulin resistance in mice with metabolic dysfunctions. Sun et al.^{8,9} reported that adipose grafts can secrete a considerable amount of growth factors that promote angiogenesis and facilitate wound healing. This mechanism contributes to reducing local inflammation and shortens the healing duration in diabetic murine models.

The pathogenesis of PAD is multifaceted, but restoring blood supply to the ischemic region remains the primary therapeutic objective¹⁰. Patients with PAD often suffer from ischemic tissue necrosis, impaired wound healing, and various associated symptoms. Therefore, the treatment of PAD involves not only the reconstruction and recanalization of ischemic blood vessels but also the modulation of inflammatory responses and the facilitation of epithelial tissue repair in wounds. Adipose tissue is recognized as the most extensive endocrine organ in the human body. Previous studies have confirmed that adipose tissue is closely associated with angiogenesis and inflammation¹¹. A considerable number of cytokines produced by adipose tissue participate in regulating glucose homeostasis, modulating inflammatory responses, and stimulating fibroblast proliferation. Leptin, the first identified adipokine, is capable of inhibiting insulin action and further aggravating insulin resistance in diabetic conditions¹²; Adiponectin promotes the release of nitric oxide in vascular endothelial cells, downregulates inflammatory factors and cytokines associated with endothelial injury, thereby reducing inflammation¹³; In contrast, chemokines intensify inflammation and play a role in the development of insulin resistance¹⁴. Moreover, fat transplantation is a well-established technique that has been employed in clinical practice for over a century. Hence, adipose tissue transplantation could serve as a promising modality for treating or alleviating the symptoms of PAD.

This study established a diabetic lower limb ulcer mouse model to simulate PAD, and normal mouse BAT was transplanted into the ischemic lower limb. Furthermore, the recovery of blood flow and the necrosis at the ischemic site were observed in the transplanted mice. In addition, changes in the body weight and blood glucose levels of the mice were monitored. At 21 days post-transplantation, the gastrocnemius muscle of the mice was harvested to observe histopathological changes and assess the level of inflammation, the levels of angiogenesis-related factors, and the polarization of macrophages. This research aimed to illustrate the function of BAT transplantation in alleviating ischemic injury associated with PAD and explore the mechanisms.

Materials and methods

Experimental animals and grouping

Thirty male C57BL/6J mice (weight: 18–22 g) were purchased from Shanghai SLAC Laboratory Animal Co., Ltd. The mice were reared in the Center for Basic and Translational Research Animal Laboratory at the Second Affiliated Hospital Zhejiang University School of Medicine (temperature, 22 ± 2 °C; humidity, 40–70%; 12/12 h dark/light cycle) with unrestricted access to food and water during the experiment. The protocol of the animal study was reviewed and approved by the Laboratory Animal Ethics Committee of the Second Affiliated Hospital of Zhejiang University School of Medicine (Year 2024, Approval No. 345). In our research, intraperitoneal administration of pentobarbital sodium was used to induce anesthesia and euthanasia, with the euthanasia dose being three times the anesthetic dose. All methods and experiments in this research were performed in accordance with the ARRIVE guidelines and relevant regulations.

The mice were randomly divided into three groups, namely the Normal group (Sham group), the Model group (Diabetic lower limb ulcer model group), and the BAT group (BAT transplantation group), with each group comprising ten individuals. All mice in each group were subjected to laser doppler, glucose level, and body weight monitoring. To minimize intergroup variations, only samples from the Model and BAT group with the necrosis scores (refer to below) of 1, 2, and 3 were subjected to WB analysis (one sample per score), immunofluorescence, and ELISA assays (five randomly selected samples). In the Normal group, three samples were randomly chosen for WB analysis, while five were subjected to immunofluorescence and ELISA analyses.

Antibodies and reagents

UCP1 Polyclonal antibody (23673-1-AP), VEGFA Polyclonal antibody (19003-1-AP), PDGFB Polyclonal antibody (AF0240), TGF-β Polyclonal antibody (21898-1-AP), TNF-α Monoclonal antibody (60291-1-LG), Arginase-1 Polyclonal antibody (16001-1-AP), and CoraLite488-conjugated Anti-Rabbit IgG (SA00014-2) were procured from Proteintech (Chicago, USA); FGF21 Rabbit Polyclonal Antibody (AF6897) and GDF15 Rabbit Polyclonal Antibody (AF6975) were procured from Beyotime (Shanghai, China); Recombinant Anti-CD31 antibody (GB15063), Anti-α-SMA Rabbit pAb (GB111364), Anti-CD68 Rabbit pAb (GB113109-100), and Anti-CD163 Rabbit pAb (GB11340-100) were procured from Servicebio (Wuhan, China); IL-6 Polyclonal antibody (IPB0062) and IL-1β Polyclonal antibody (IPB0002) were procured from BAIJIA; IL-1β (BPE20533), IL-10 (BPE20005), TNF-α (BPE20220), and Arg-1 (BPE20450) ELISA Kit were procured from Lengdon (Shanghai, China); IL-10 Rabbit pAb (bs-0698) was procured from Bioss (Beijing, China); DAPI (S19119) was procured from Yuanze (Shanghai, China).

Establishment of diabetic lower limb ulcer in mice

Establishment of diabetic mice model

Prior to modeling, the mice were fasted for 8 h and received an intraperitoneal injection of streptozotocin (STZ) dissolved in citrate buffer at pH 4.5. Continuous administration was carried out for three days, with dosages of 80 mg/kg on the first day, 60 mg/kg on the second day, and 80 mg/kg on the third day. After one week of continuous feeding, blood samples were collected from the tail to measure blood glucose levels (repeated three times). A random blood glucose level $> 16 \text{ mmol/L}$ or a fasting blood glucose level $\geq 11.1 \text{ mmol/L}$ indicated the successful establishment of the diabetic mouse model.

Establishment of lower limb ulcer model in diabetic mice

Once the diabetic mouse model was successfully established, a diabetic lower extremity ulcer model was constructed by high ligation of both the femoral artery and vein, followed by disconnection of the femoral artery. Mice were anesthetized by intraperitoneal administration of 0.1% pentobarbital sodium at 0.1 mL per 10 g of body weight. Muscle relaxation and limb inactivity were confirmed by a lack of response when the whiskers were stimulated. The mice were immobilized on the operating table, and the fur on the lower limbs was removed by using depilatory cream. Subsequently, the skin was sterilized with 75% alcohol, and the right lower limb was designated as the surgical area. Under a stereomicroscope, the skin over the inguinal region was incised to expose the femoral artery while separating the veins and nerves. The femoral arteries and veins were ligated near the knee joint using 4–0 silk sutures. The upper end of the arterial bifurcation was also ligated accordingly, and the artery was severed using ophthalmic scissors. The bleeding was controlled by applying pressure for 5 min, the skin was sutured with 6–0 thread, and the area was disinfected with 75% alcohol. Subsequently, the mice were placed on a constant temperature electric blanket at 37 °C for 30 to 60 min until they woke up.

Preparation of BAT grafts

C57BL/6J male mice (18–22 g) were anesthetized by intraperitoneal injection of 0.1% pentobarbital sodium. Following anesthesia, the mice were fixed and the heart and a part of the liver were exposed. Firstly, a 5 mL syringe needle was inserted gently into the left ventricle, followed by an incision in the right atrial appendage. Perfusion with normal saline was conducted until the liver appeared white. BAT was harvested subcutaneously from the scapular region of the mice using a sterile blade. Fifty milligrams of each specimen were collected as fat grafts and temporarily stored at a low temperature before transplantation.

BAT transplantation

The BAT group received simultaneous BAT transplantation during the ischemic surgical procedure. Following surgery, the skin incision was sutured, and the operative site was irrigated with normal saline. In contrast, the model control group only underwent ischemic surgery to establish a diabetic lower limb ulcer model, while the normal control group underwent a sham operation.

Evaluation of limb necrosis and laser doppler monitoring

The body weight and blood glucose levels of the mice were evaluated weekly. Limb ischemia was observed on the 14th day after ischemic surgery. The following reference scores were used for evaluation:

- 0: No significant changes in skin color or temperature;
- 1: necrosis was confined to the toes without toe shedding
- 2: necrosis was confined to the foot, with or without toe shedding
- 3: necrosis extended to the lower leg, with toe loss
- 4: necrotic area progressed to the thigh and above, requiring amputation

Laser Doppler flow imaging was utilized to dynamically monitor changes in blood flow in the lower limbs of mice in all groups before and after ischemic surgery and on postoperative days 3, 7, 14, and 21. Each mouse was monitored for approximately 20 s. The ratio of mean perfusion in the ischemic limb to that in the normal limb was statistically analyzed. Following anesthesia, the mice were positioned on a 37 °C thermostatic pad to maintain their body temperature. Once circulation and respiration stabilized, the mice were secured in a supine position on the detection pad. The unoperated left lower limb served as a reference for analyzing relative blood perfusion in the right lower limb. After the test, the mice were placed in a prone position on a 37 °C constant temperature electric blanket for 30 to 60 min until they woke up.

Western blot analysis

Twenty-one days post-surgery, the adductor and gastrocnemius muscle tissue from the right hind limb (surgical limb) were collected. The tissues were cleansed, washed with precooled PBS, sliced into 1 mm × 1 mm blocks, and a tenfold volume of RIPA lysis buffer was added. The mixture was homogenized thoroughly on ice. After lysis, the tissue was centrifuged at 12,000 rpm for 10 min at 4 °C, and the supernatant was transferred to a new centrifuge tube. The BCA assay was performed to quantify the protein concentration in each group¹⁵. Loading buffer was added, and the samples were denatured by heating in a metal bath at 100 °C. Thereafter, protein samples were separated using 12% sodium dodecyl sulfate-polyacrylamide gel electrophoresis (SDS-PAGE) and transferred onto polyvinylidene fluoride membranes. The membranes were blocked with skim milk powder for 2 h at room temperature and incubated overnight at 4 °C with primary antibodies (UCP1, VEGF-A, FGF21, GDF15, and PDGF- β polyclonal antibodies). Subsequently, the membranes were washed three times for 5 min each with PBST, followed by incubation with anti-rabbit horseradish peroxidase-conjugated secondary antibodies (goat anti-rabbit IgG) for one hour at room temperature. After washing three times for 5 min each

with PBST, unbound secondary antibody proteins were visualized using autoradiography. Densitometric analysis was conducted using ImageJ, and the relative band densities of the proteins were normalized to those of GAPDH and adjusted against normal control samples.

Histology staining and Immunofluorescence

Twenty-one days post-surgery, the gastrocnemius muscle tissue from the right hind limb (surgical limb) of mice was collected and fixed in a 10% paraformaldehyde solution. Muscle tissues of each group were embedded in paraffin and sectioned into 3 μm slices. Hematoxylin and eosin staining was performed to evaluate the pathological changes in muscle tissue. For immunofluorescence, sections were fixed with 4% paraformaldehyde for 20 min and treated with Triton X-100 for another 20 min. Non-specific binding sites were blocked for 1 h by using 5% BSA in PBS. Subsequently, the samples were incubated overnight with antibodies against α -SMA, CD31, CD68, CD163, TGF- β , TNF- α , IL-1 β , IL-6, IL-10, and Arg-1. Then, immunostaining was performed using CoraLite488-conjugated goat anti-rabbit antibodies for 1 h at room temperature, followed by nuclear counterstaining with DAPI. Images were captured using a fluorescence microscope and analyzed with NIS-Elements software.

ELISA assay

The gastrocnemius muscle tissue from the right hind limb (surgical limb) of mice was collected 21 days after the surgery. The tissue homogenate was prepared by using a high-speed homogenizer under low-temperature conditions. Following centrifugation, the supernatant was collected, and the levels of TNF- α , IL-1 β , IL-10, and Arg-1 in the supernatant were quantified according to the protocols described in the ELISA kit.

Statistical analysis

The data acquired in this study were statistically analyzed using GraphPad Prism 8.0 (GraphPad, United States) and presented as means \pm standard deviation. Pairwise comparisons between groups were analyzed by the Student's t-test, while comparisons between multiple groups were analyzed by One-way ANOVA. In this study, $P < 0.05$ was considered statistically significant.

Results

Changes in blood glucose level and body weight of mice

After the STZ injection, the weight and blood glucose levels of the mice were monitored weekly. Blood glucose levels reached the diabetic threshold by the second week. Blood glucose was allowed to stabilize for one week, and the diabetic lower limb ulcer model was established. Subsequently, BAT transplantation was performed. Furthermore, the alterations in blood flow 21 days post-surgery were relatively limited, and the necrotic damage was irreversibly established. Consequently, the experiment was concluded 21 days after the surgery. (Fig. 1A)

Weight change: The weight of mice in the Normal group increased gradually. In contrast, the weight of the mice in the Model group and the BAT group declined after STZ injection. More significant weight loss was observed following ischemic surgery, with the weight showing an increasing trend during the second week. The weight changes in all three groups were similar. (Fig. 1B)

Blood glucose change: After administration of STZ, blood glucose levels increased significantly before stabilizing. Following ischemic surgery, blood glucose levels rose again but decreased two weeks after surgery. The decline was more pronounced in the BAT transplantation group compared to the Model group but the difference was not statistically significant. (Fig. 1C)

Evaluation of ischemic lower limb necrosis and changes in blood perfusion

The necrosis of the ischemic lower limb in mice was observed fourteen days after surgery. The mean necrosis score was 2.3 points in the model group and 1.9 points in the BAT transplantation group (Table 1). The distributions of necrosis scores between the two groups did not reach statistical significance (the Mann Whitney U test result: $p = 0.2217 > 0.05$). However, Among mice with lower limb ischemia, necrosis was mainly localized to the soles of the feet in the BAT group, with some toes presenting necrosis and exfoliation. In contrast, necrosis in the model group had advanced to the shank, with most toes showing signs of necrosis and exfoliation, and even some cases of gangrene. (Figure 2A and B)

The lower limb blood flow was monitored by a laser Doppler flowmeter on the day of ischemic surgery, as well as before the surgery and on the 3rd, 7th, 14th, and 21st days after the procedure. Our findings show that, compared to the model group, the recovery of lower limb blood perfusion in the BAT group was significantly better on postoperative days 7 and 14. Subsequently, both groups progressively returned to normal levels. (Figure 2C and D)

BAT was successfully transplanted into mice with diabetic lower limb ulcers

Mitochondrial uncoupling protein 1 (UCP1) is highly expressed in BAT. Twenty-one days post-surgery, UCP1 expression in the gastrocnemius muscle of mice from each group was assessed using Western blotting. The results indicated that UCP1 protein levels were significantly elevated in the BAT group compared with normal mice (Fig. 3A and C; $P < 0.05$). In contrast, no significant changes were detected between the model group and normal mice. These findings confirmed the therapeutic efficacy of BAT transplantation in diabetic mice with lower limb ulcers.

Fibroblast growth factor 21 (FGF21) is predominantly expressed in skeletal muscle, BAT, and other tissues, and plays a crucial role in angiogenesis. Growth differentiation factor 15 (GDF15) is synthesized by macrophages and endothelial cells¹⁶. GDF15 inhibits excessive macrophage activation and the expression of TNF- α via an autocrine negative feedback regulation mechanism¹⁷, thereby contributing to anti-inflammatory, anti-apoptotic,

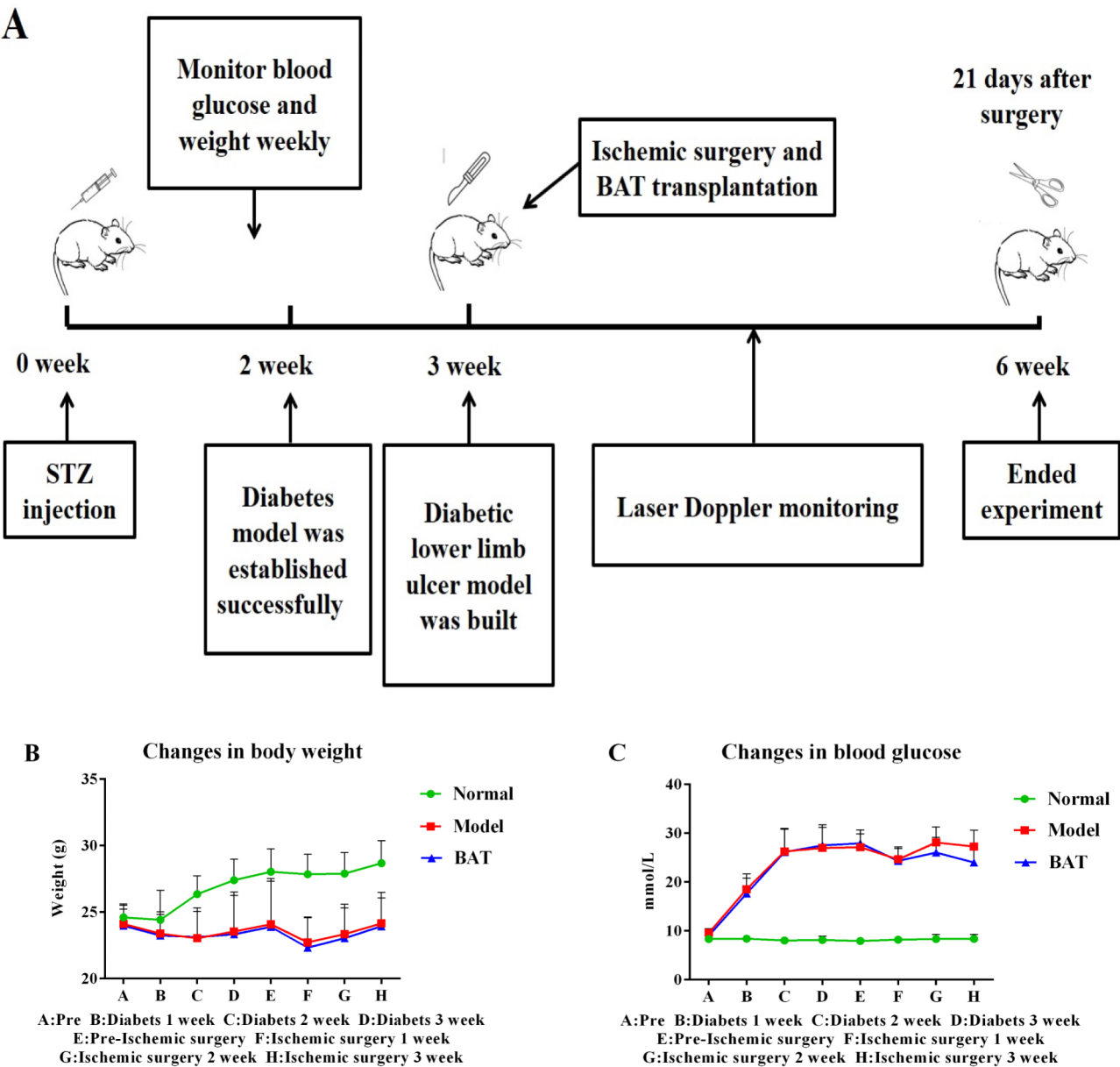


Fig. 1. (A) Fourteen days following STZ injection, the mice underwent lower limb ischemia surgery, followed by BAT transplantation; the experiment was concluded on the 21st day post-surgery. (B) Weekly weight changes. (C) Weekly blood glucose levels. Data are presented as the mean \pm SD ($n=10$).

Group	<i>n</i>	Score=0	Score=1	Score=2	Score=3	Score=4	Average
Normal group	10	9	1	0	0	0	0.1
Model group	10	0	2	4	3	1	2.3
BAT group	10	0	4	3	3	0	1.9

Table 1. Necrosis scores of mice in each group.

and antioxidant responses. Furthermore, FGF21 expression levels showed no significant differences among the groups. (Figure 3B and F; $P>0.05$). Nonetheless, the expression of GDF15 in the tissues of the BAT group was elevated, indicating that BAT transplantation may inhibit excessive macrophage activation and mitigate inflammation (Fig. 3B and G; $P<0.05$).

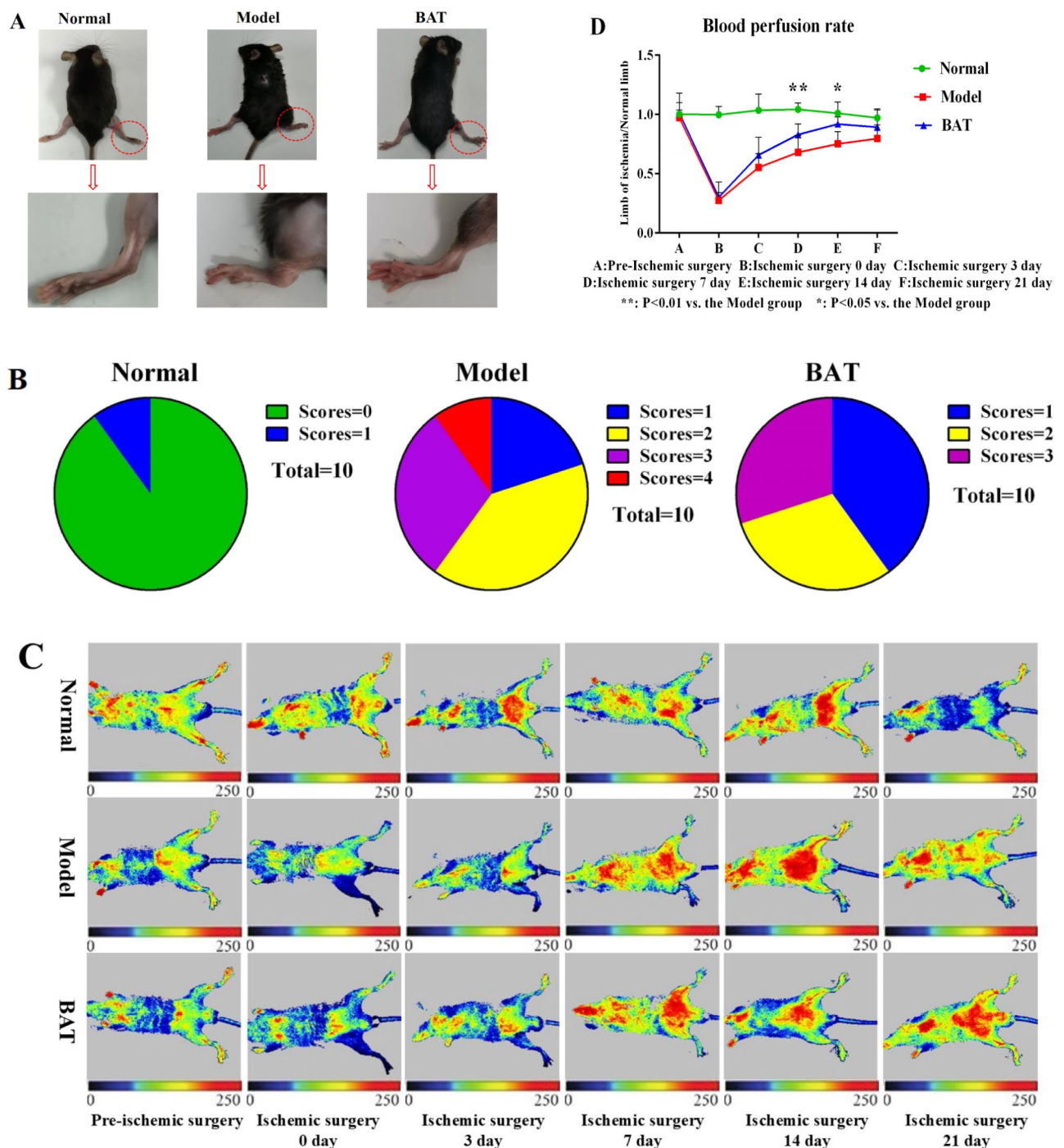


Fig. 2. (A) Ischemic necrosis was observed fourteen days post-surgery. (B) “Scores of 2, 3, and 4” indicates that the mice experienced toe shedding, with the model group exhibiting a greater extent of toe shedding compared to the BAT group ($n = 10$). (C) Changes in blood flow in the lower limbs were assessed prior to the surgery and at 0, 3, 7, 14, and 21 days post-surgery. (D) The ratio of mean perfusion in the ischemic limb to that in the normal limb was employed to evaluate the restoration of blood flow. Data are presented as the mean \pm SD ($n = 10$), ** $P < 0.01$, vs. the Model group, * $P < 0.05$, vs. the Model group.

Histopathological changes in muscle tissue of diabetic mice with lower limb ulcers following BAT transplantation

Hematoxylin-eosin staining revealed significant destruction of muscle fiber structure in mice from the Model group. The tissue exhibited a loose structure with disrupted muscle fibers, broadened muscle spaces, and an elevated number of damaged cells. In contrast, the gastrocnemius muscle tissue in the BAT group presented an

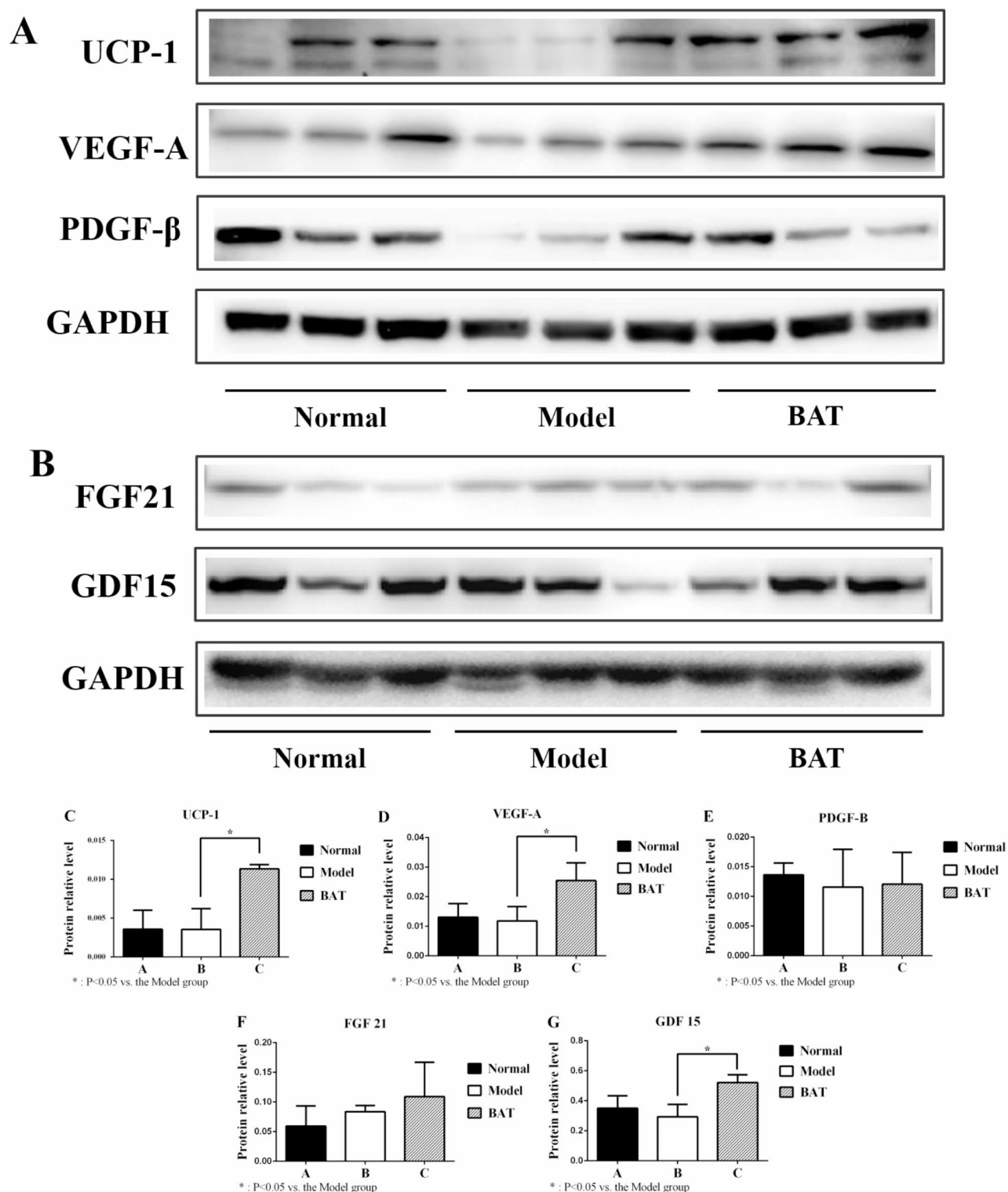


Fig. 3. (A) Protein levels of UCP1, VEGF-A, and PDGF- β from muscular tissue. (B) Protein levels of FGF21 and GDF15. (C) UCP-1 protein was highly expressed in the BAT group. (D) VEGF-A protein was highly expressed in the BAT group. (E) No significant difference in PDGF- β protein levels was found between these groups. (F) No significant difference in FGF21 protein levels was observed between these groups. (G) GDF15 protein was highly expressed in the BAT group. Data are presented as the mean \pm SD ($n = 3$), * $P < 0.05$, vs. the Model group.

intact structure, with muscle cells showing a normal shape and neat arrangement. Despite some mild muscle fiber atrophy, necrosis, and myolysis, only a minimal number of damaged cells was observed. (Fig. 4A)

Platelet endothelial cell adhesion molecule-1 (PECAM-1/CD31) and α -smooth muscle actin (α -SMA) reflect the distribution of smooth muscle cells and new arterial microvessels in tissues. Under the microscope, within fields of the same size, we observed that the expression of red fluorescein-labeled CD31 and α -SMA in the gastrocnemius muscle tissue of the BAT group was greater than that in the model group and the normal group (Fig. 4B). These findings imply that BAT transplantation can promote microvascular regeneration after injury.

The impact of BAT transplantation on angiogenesis

Vascular endothelial growth factor-A (VEGF-A) plays a pivotal role in promoting neovascularization and enhancing vascular permeability¹⁸. VEGF-A participates in the thermogenesis and angiogenesis of BAT via paracrine or autocrine mechanisms¹⁹. Overexpression of VEGF-A can give rise to brown adipose-like cells in white adipose tissue²⁰. Hence, VEGF-A expression might be correlated with the formation of BAT. In addition, platelet-derived growth factor (PDGF) assumes a crucial role in wound healing, expediting the regeneration and repair of damaged tissues by stimulating the proliferation and migration of fibroblasts, smooth muscle cells, and other cells. The expression of PDGF-B is not only associated with angiogenesis but also mirrors wound healing. The expression levels of VEGF-A and PDGF- β in the gastrocnemius muscle of mice from each group were determined using Western blot analysis. The results showed that the protein levels of VEGF-A were significantly elevated in the BAT group compared to the Model group (Fig. 3A and D; $P < 0.05$). However, no significant difference was observed between the Model group and the Normal group. Decreased protein levels of PDGF- β were observed in both the BAT group and the Model group compared to the Normal group. Nonetheless, no significant differences were observed between these groups. Furthermore, the protein levels of PDGF- β in the BAT group were marginally elevated relative to those in the model group; still, no statistically significant difference was detected (Fig. 3A and E; $P > 0.05$).

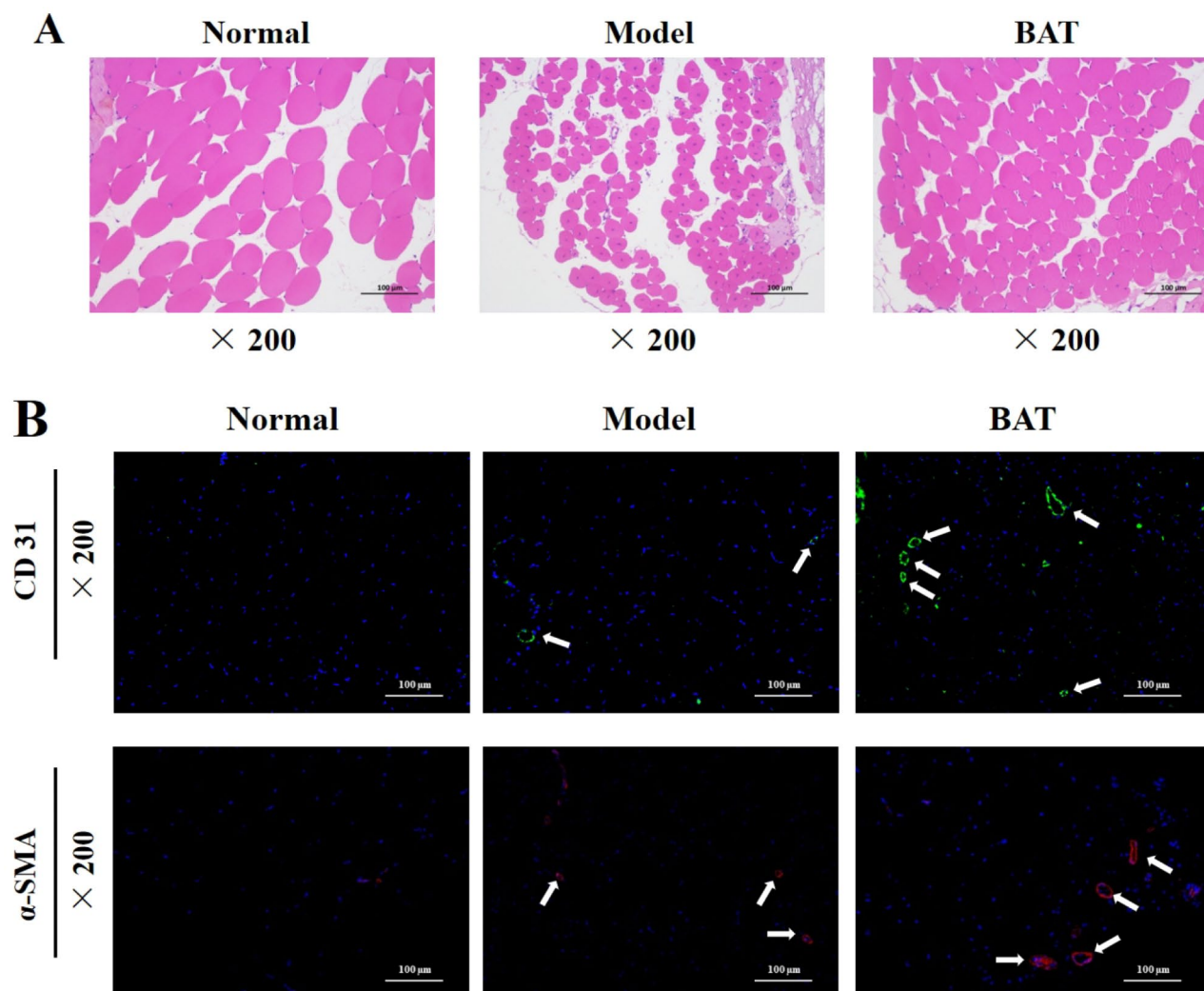


Fig. 4. (A) Muscle tissue hematoxylin-eosin staining (×200). (B) CD31 and α -SMA immunofluorescence staining (CD31 and α -SMA staining is red, DAPI staining is blue, arrows indicate new blood vessels, ×200).

BAT transplantation mitigates excessive inflammation after ischemic injury

The levels of pro-inflammatory cytokines IL-1 β , IL-6, and TNF- α , as well as anti-inflammatory cytokines IL-10 and Arg-1, were evaluated using immunofluorescence staining 21 days after surgery. The results demonstrated significantly raised expression of IL-1 β , IL-6, and TNF- α in the tissues of model mice compared to those of normal mice. Conversely, following BAT transplantation, a marked reduction in the expression levels of IL-1 β , IL-6, and TNF- α was observed relative to the model group, which was accompanied by an increase in the expression levels of IL-10 and Arg-1 (Fig. 5A, B, C, E and F). Furthermore, the concentrations of pro-inflammatory cytokines IL-1 β and TNF- α , as well as anti-inflammatory cytokines IL-10 and Arg-1 in tissue, were quantified using ELISA. Notably, M1 macrophages were primarily responsible for the secretion of IL-1 β and TNF- α , whereas IL-10 and Arg-1 were predominantly secreted by M2 macrophages. The results indicated significantly reduced levels of IL-1 β and TNF- α in the BAT group compared to the model group, accompanied by markedly elevated levels of IL-10 and Arg-1 (Fig. 5G, H, I and J; $P < 0.05$). Therefore, BAT transplantation effectively attenuated inflammatory responses and promoted the polarization of M2 macrophages within tissues.

Transforming growth factor beta (TGF- β) plays an essential role in promoting the proliferation of mesenchymal cells, which leads to extracellular matrix production and mediates the fibrotic response within tissues. This factor is significantly upregulated in mesenchymal cells during chronic inflammatory conditions. Immunofluorescence staining revealed elevated TGF- β levels in the tissues of model mice compared to those in normal mice, which decreased following BAT transplantation (Fig. 5D). These findings indicate that elevated TGF- β levels may be associated with sustained chronic inflammation.

Impact of BAT transplantation on macrophage polarization following ischemic injury

CD68 is recognized as a marker for M1 macrophages, whereas CD163 serves as a marker for M2 macrophages. Ischemic injury resulted in elevated CD68 expression in tissues; however, BAT transplantation effectively decreased CD68 expression while increasing CD163 expression (Fig. 6). These results indicated that ischemic injury promotes M1 polarization while inhibiting M2 polarization of macrophages in diabetic mice, which was reversed by BAT transplantation.

Discussion and conclusion

The management of PAD primarily encompasses pharmacological interventions, surgical procedures, and stem cell therapies. Owing to the intricate etiology and unclear pathogenesis of PAD, effective pharmacological agents specifically targeting this condition are currently lacking. Existing medications primarily focus on mitigating symptoms rather than targeting the underlying cause. Endovascular intervention for reconstructing affected vessels is a commonly used surgical approach for PAD. Nevertheless, the surgery poses a higher risk for patients with severe diabetes complications and the elderly. Stem cell therapy represents a significant area of research in the management of PAD but has yet to be applied in clinical practice. Fat grafting is a time-honored clinical technique with several advantages, including abundant availability, easy harvesting, and low immune rejection in autologous transplantation. Sun et al.⁸ demonstrated that fat grafts can secrete a substantial array of growth factors that facilitate angiogenesis and promote wound healing. In contrast to the singular target of pharmacological interventions, fat transplantation offers a broader range of therapeutic targets. Adipose tissue not only contains adipose-derived stem cells but also secretes various adipokines, enhancing its functional potential. Furthermore, autologous fat grafting is considered safer than stem cell therapy. Consequently, fat grafting may represent a viable treatment option for PAD. Currently, research on fat transplantation for the treatment of PAD and diabetic foot remains predominantly in the preliminary exploratory phase. There is a significant lack of in-depth mechanistic studies, as well as robust clinical validation of efficacy and safety. In 2019, K.C. Moon et al.²¹ treated 10 patients with ischemic diabetic foot ulcers using autologous adipose-derived stromal vascular fraction cells. The treatment significantly increased transcutaneous oxygen partial pressure and skin microvascular blood flow. Roberto Lonardi et al.²² harvested microfragmented adipose tissue from patients with mild lower limb amputations and injected it into the peristomal areas around the amputation sites. After 6 months, 80% of the treated residual limbs achieved successful healing. Overall, fat transplantation has shown some clinical efficacy as an adjuvant therapy for diabetic foot, but further studies are needed.

Adipose tissue in humans and mammals is classified into two distinct types: WAT and BAT. Fruhbeck et al.²³ reported the presence of activated BAT in adults, as evidenced by positron emission tomography (PET) imaging in 2009. BAT is the primary site of adaptive non-shivering thermogenesis in the body. Its thermogenic activity is regulated by sympathetic innervation, which involves UCP1. UCP1 is located in the inner mitochondrial membrane and serves as a hallmark protein of BAT²⁴. As opposed to WAT, BAT plays a pivotal role against obesity and metabolic disorders by utilizing glucose and lipid substrates for energy expenditure²⁵. Stanford⁵ demonstrated that BAT transplantation enhances glucose homeostasis and insulin sensitivity in the body. In STZ-induced type 1 diabetic mice, BAT transplantation was found to not only improve glucose metabolism but also mitigate tissue inflammation and reverse the clinical manifestations of diabetes²⁶. Targeted disruption of the UCP1 gene in mice has been shown to specifically inhibit the thermogenic function of BAT without inducing body weight gain. Conversely, genetic ablation of BAT can result in obesity, diabetes mellitus, and hyperlipidemia^{27,28}. This discovery indicates that beyond thermogenesis, BAT also plays a significant role in modulating human metabolism. Furthermore, BAT facilitates the repair of muscle injuries. Bryniarski et al.²⁹ revealed that BAT transplantation into damaged muscle tissues enhances muscle regeneration, as evidenced by in vivo transplantation experiments. Moreover, several studies have confirmed the presence of UCP1-positive cells (marker gene for BAT) in muscle tissue during skeletal muscle regeneration^{30,31}. Although the origin and function of these cells remain unknown, their role in facilitating muscle regeneration has been validated. These findings confirm that BAT plays a distinct role in regulating the body's metabolic functions and facilitating skeletal muscle regeneration. The current study proposes that BAT represents a more effective target for fat

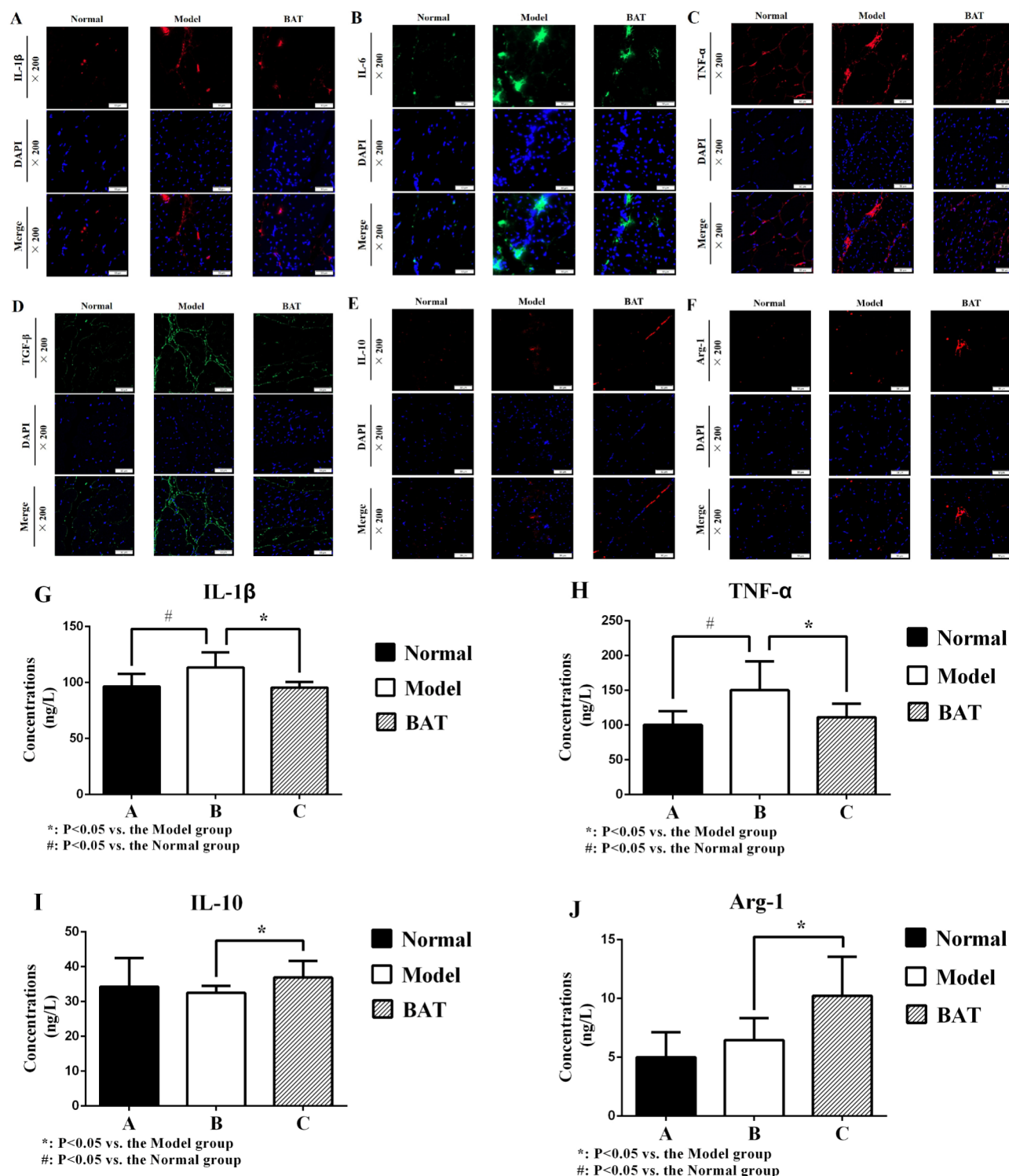


Fig. 5. (A) IL-1 β immunofluorescence staining (IL-1 β staining is red, DAPI staining is blue, $\times 200$). (B) IL-6 immunofluorescence staining (IL-6 staining is green, DAPI staining is blue, $\times 200$). (C) TNF- α immunofluorescence staining (TNF- α staining is red, DAPI staining is blue, $\times 200$). (D) IL-6 immunofluorescence staining (TGF- β staining is green, DAPI staining is blue, $\times 200$). (E) IL-10 immunofluorescence staining (IL-10 staining is red, DAPI staining is blue, $\times 200$). (F) Arg-1 immunofluorescence staining (Arg-1 staining is red, DAPI staining is blue, $\times 200$). (G–J). The content of IL-1 β , IL-6, IL-10, and Arg-1 in tissue homogenates. Data are presented as the mean \pm SD ($n = 5$), * $P < 0.05$, vs. the Model group, # $P < 0.05$, vs. the Normal group.

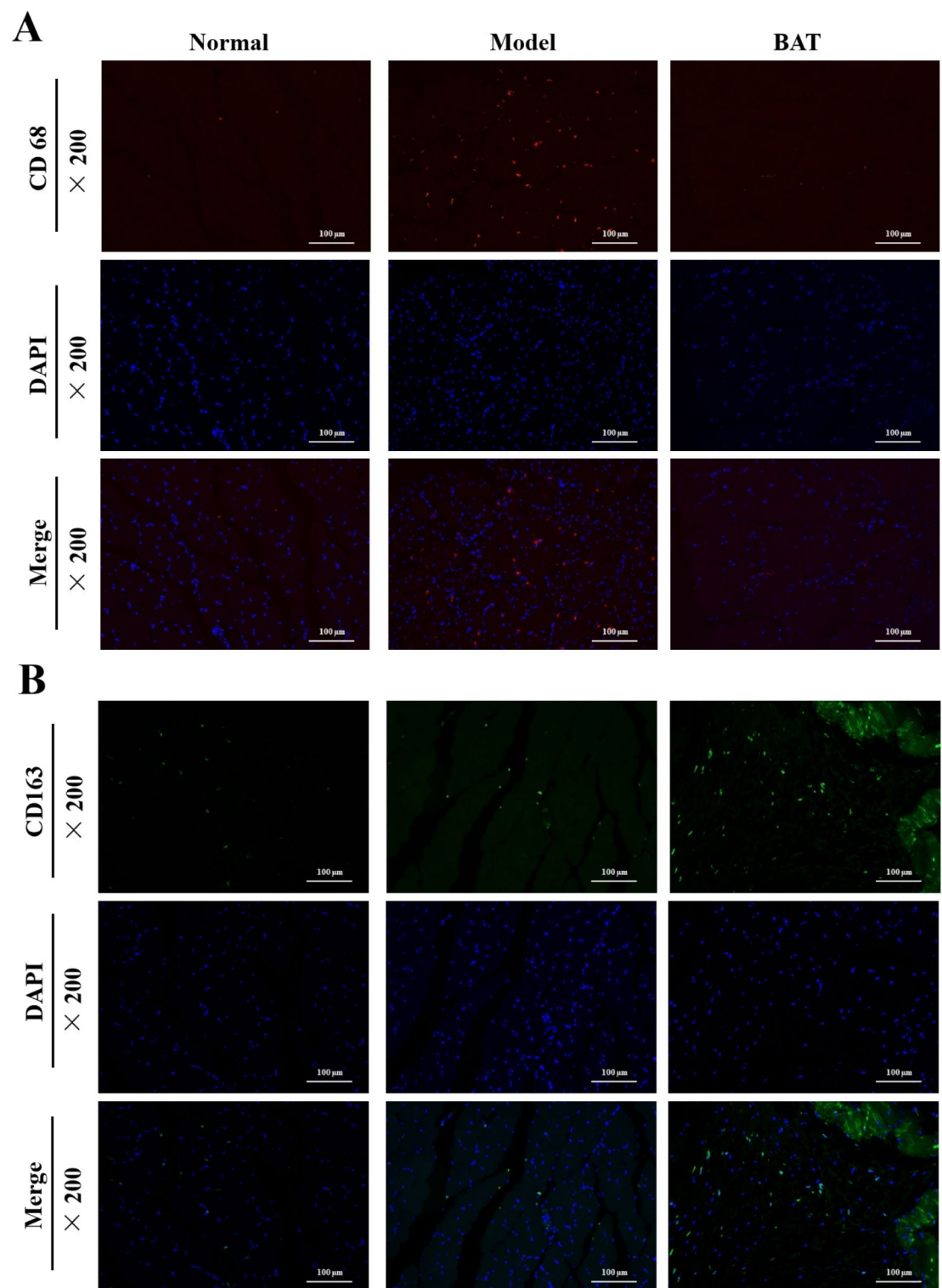


Fig. 6. (A) CD68 immunofluorescence staining (CD68 staining is red, DAPI staining is blue, $\times 200$). (B) CD163 immunofluorescence staining (CD163 staining is green, DAPI staining is blue, $\times 200$).

grafting compared to WAT. Nonetheless, fat transplantation is primarily limited by the low survival rate of adipose tissue and many complications. Mitigating tissue necrosis following fat transplantation is essential for enhancing the success rate of this procedure. Qiu et al.³² reported the browning of adipose tissue during fat grafting. In addition, the incorporation of exosomes derived from adipose stem cells during fat transplantation can promote adipose browning and enhance the survival rate of the graft³³. Cai's study³⁴ demonstrated higher retention rates with BAT compared to WAT, with the grafts exhibiting more complete tissue structure and

enhanced vascularization. A higher survival rate of adipose tissue was observed with direct transplantation of BAT compared to WAT, lending support to BAT being the preferred choice for transplantation. In the present study, newly adult mice were selected as BAT donors to obtain samples with enhanced biological activity. Simultaneously, the *in vitro* duration of adipose tissue was minimized to ensure the activity of BAT grafts.

This study employed a diabetic lower limb ulcer mouse model to simulate PAD in patients with diabetic foot. Diabetic foot ulcer (DFU) involves multiple pathogenic factors such as vascular pathology, neuropathy, infection, and so on³⁵. The combination of high glucose microenvironment and microcirculatory injury contributes to the development of PAD and tissue ischemia, thereby resulting in tissue damage and an inflammatory response. Furthermore, elevated blood glucose levels perpetuate a chronic and severe inflammatory state that inhibits angiogenesis and tissue repair, leading to diabetic foot. The model used in this study effectively simulated this process, representing the advantages and innovations of this animal model. Nevertheless, this model employs surgical techniques to induce ischemia, representing an acute vascular injury. In contrast, the mouse model has certain limitations when compared to human PAD. Firstly, human diabetic vascular disease is predominantly attributed to atherosclerosis, a chronic vascular condition. Secondly, this model utilized a type 1 diabetes mouse model, while human diabetic vasculopathy typically arises from type 2 diabetes. Future research should focus on key areas limiting the application of the model, such as surgical injuries compromising the accuracy of the model. The changes in blood perfusion rate reflect vessel regeneration and remodeling in the limb following ischemic injury. At equivalent recovery time, mice receiving BAT transplantation exhibited significantly improved outcomes compared to those without such intervention. Mice exhibit a superior recovery capacity compared to humans, with ischemic regions gradually recovering. Conversely, necrotic areas typically do not recover. Consequently, necrosis was evaluated, and a higher degree of necrosis was found closer to the proximal end. In mice with grafting, necrosis was typically localized to the foot, whereas the necrosis extended to above the ankle in nongrafted mice.

Although the pathogenesis of PAD is poorly understood, it is primarily associated with chronic inflammation, delayed wound healing, and dysregulation of angiogenesis. This study proposes a reciprocal influence and interaction among these three factors. Under physiological conditions, a well-regulated inflammatory response can promote effective wound healing. However, individuals with diabetes frequently dysregulated glucose and lipid metabolism, which can synergistically enhance the release of inflammatory mediators and promote the infiltration of macrophages and other immune cells, resulting in a state of chronic inflammation within the body³⁶. Concurrently, the high-glucose microenvironment impairs the chemotactic aggregation capabilities of neutrophils and macrophages, resulting in elevated levels of inflammatory mediators³⁷. A prolonged inflammatory response triggers the release of proteolytic enzymes that degrade the nascent extracellular matrix, resulting in localized edema and impeding wound healing³⁸. Therefore, an appropriate inflammatory response promotes wound healing. However, the inflammatory response is dysregulated in diabetic patients. Chronic inflammatory response impairs angiogenesis and wound healing, serving as a critical factor in the pathogenesis of PAD and DFU. In this study, increased expressions of inflammatory factors IL-1 β and TNF- α were detected, as well as decreased expression of anti-inflammatory factor IL-10, and reduced levels of angiogenesis-related proteins VEGF and PDGF in the ischemic tissue of model mice. Ischemia may trigger an exaggerated inflammatory response in diabetic mice, which impairs angiogenesis, thereby hindering the restoration of blood supply and resulting in necrosis. Following BAT transplantation, a significant reduction in inflammatory markers was achieved in ischemic tissue, accompanied by an elevated expression of angiogenesis-related proteins. Consequently, blood supply was restored and necrosis was ameliorated. BAT transplantation may mitigate the excessive inflammatory response following ischemic injury, enhance angiogenesis, and restore tissue repair functions of the body.

Extended exposure to a hyperglycemic environment negatively impacts the functionality of inflammatory cells, including macrophages and neutrophils. As highly plastic cells, macrophages undergo phenotypic and morphological differentiation in response to microenvironmental stimuli, such as pathogen invasion, tissue damage, and metabolic disorders, thereby secreting a variety of chemokines and cytokines³⁹. This process is referred to as macrophage polarization. A high glucose microenvironment promotes the polarization of M1 macrophages while inhibiting their transition to the M2 phenotype, shifting the balance towards chronic inflammation in wounds and impeding the healing process⁴⁰. M1 macrophages primarily synthesize and secrete pro-inflammatory cytokines, such as IL-1 and IL-6, which mediate inflammatory responses. In contrast, M2 macrophages produce cytokines, such as IL-10, that play a critical anti-inflammatory role. In the early stages of healing, monocytes are recruited and differentiate into pro-inflammatory M1 macrophages at the wound site, activating the inflammatory response. Upon entering the proliferation phase, M1 macrophages are polarized into anti-inflammatory M2 macrophages that inhibit inflammation and facilitate tissue repair. In this study, an increased expression of the M1 macrophage marker CD68 was observed in ischemic tissues of diabetic mice with lower limb ulcers, whereas the expression of M2 markers Arg-1 and CD163 were downregulated. Furthermore, tissue homogenates revealed elevated levels of inflammatory cytokines IL-1 β , IL-6, and TNF- α secreted by M1 macrophages, alongside a reduction in the anti-inflammatory cytokine IL-10 produced by M2 macrophages. These results indicated that diabetes inhibits the polarization of M1 macrophages to the M2 phenotype, thereby maintaining ischemic tissue in a prolonged inflammatory state. However, BAT transplantation effectively reversed this trend, facilitating the transition from M1 macrophages to the M2 phenotype and reducing tissue inflammation levels. Therefore, high glucose levels may disrupt the balance of macrophage polarization, leading to chronic inflammation that inhibits angiogenesis in injured tissues and results in ischemic necrosis. BAT transplantation facilitates the polarization of M1 macrophages to the M2 phenotype, mitigates the chronic inflammatory response, enhances angiogenesis in ischemic tissue, and accelerates healing.

Despite the high biocompatibility associated with autologous fat transplantation, our experimental findings revealed that a subset of mice developed severe infections post-transplantation, resulting in cyst formation

and necrosis at the graft site, and even gangrene. These adverse outcomes may be attributed to inflammation or infection from liquefied necrotic adipose tissue or could potentially reflect inadequacies in our surgical technique. Consequently, several critical issues must be addressed prior to the clinical application of BAT transplantation: (1) the low survival rate of transplanted BAT; (2) severe infections due to ischemic necrosis and subsequent liquefaction of the transplanted BAT; (3) surgical and anesthetic risks; (4) the challenge of obtaining sufficient quantities of BAT in adult patients. Studies have demonstrated that the transplantation of platelet-rich plasma (PRP) at an appropriate concentration in conjunction with adipose tissue yields superior outcomes compared to fat transplantation alone⁴¹. Furthermore, Zhu et al.³³ found that incorporating exosomes derived from adipose stem cells during fat transplantation can enhance adipose browning and improve the survival rate of transplanted adipose. The approach provides an effective strategy for enhancing the survival rate of BAT grafts.

In this study, BAT transplantation was found to facilitate the polarization of M1 macrophages to the M2 phenotype, inhibit chronic inflammation, and promote angiogenesis while accelerating the healing of ischemic tissues. This may represent only one of the mechanisms through which BAT transplantation ameliorates PAD and warrants further investigation. Furthermore, the combined transplantation of BAT presents a viable approach to enhance transplantation success rates and mitigate infection risks, representing one of our future research directions.

Data availability

The datasets used and/or analysed during the current study available from the corresponding author on reasonable request.

Received: 1 December 2024; Accepted: 5 March 2025

Published online: 14 March 2025

References

1. Soyoye, D. O. et al. Diabetes and peripheral artery disease: A review. *World J. Diabetes*. **12** (6), 827–838 (2021).
2. Argentero, A. et al. History of the diagnosis and treatment of critical limb ischemia and diabetic foot. *Semin Vasc. Surg.* **31** (2–4), 25–42 (2018).
3. Rice, J. B. et al. Burden of diabetic foot ulcers for medicare and private insurers. *Diabetes Care* **37**, 651–658 (2014).
4. Lu Ting, L., Amin, J., Qihui & Zhang Ling. Research advances on the role of adipokines in diabetic peripheral arterial diseases. *Chin. J. Burns Wounds*. **40** (05), 495–500 (2024).
5. Stanford, K. I. et al. Brown adipose tissue regulates glucose homeostasis and insulin sensitivity. *Clin. Invest.* **123** (1), 215–223 (2013).
6. Liu, X. et al. Brown adipose tissue transplantation reverses obesity in Ob/Ob mice. *Endocrinology* **156** (7), 2461–2469 (2015).
7. Payab, M. et al. Brown adipose tissue transplantation as a novel alternative to obesity treatment: a systematic review. *Int. J. Obes. (Lond)*. **45** (1), 109–121 (2021).
8. Sun, M. et al. Adipose extracellular matrix/stromal vascular fraction gel secretes angiogenic factors and enhances skin wound healing in a murine model. *Biomed. Res. Int.* **2017**, 3105780 (2017).
9. Villarroja, F. et al. Brown adipose tissue as a secretory organ. *Nat. Rev. Endocrinol.* **13** (1), 26–35 (2017).
10. Schaper, N. C. et al. Practical guidelines on the prevention and management of diabetic foot disease. *Diabetes Metab. Res. Rev.* **36** (S1), e3266 (2020).
11. Gorgun, C. et al. Role of extracellular vesicles from adipose tissue and bone Marrow-Mesenchymal stromal cells in endothelial proliferation and chondrogenesis. *Stem Cells Transl. Med.* **10** (12), 1680–1695 (2021).
12. Stefanakis, K. et al. Leptin physiology and pathophysiology in energy homeostasis, immune function, neuroendocrine regulation and bone health. *Metabolism* <https://doi.org/10.1016/j.metabol.2024.156056> (2024).
13. Tilg, H. et al. Adipokines: masterminds of metabolic inflammation. *Nat. Rev. Immunol.* <https://doi.org/10.1038/s41577-024-01103-8> (2024).
14. Neves, K. B. et al. Chemerin receptor Blockade improves vascular function in diabetic obese mice via redox-sensitive and Akt-dependent pathways. *Am. J. Physiol. Heart Circ. Physiol.* **315** (6), 1851–1860. <https://doi.org/10.1152/ajpheart.00285.2018> (2018).
15. Smith, P. K. et al. Measurement of protein using bicinchoninic acid. *Anal. Biochem.* **150** (1), 76–85 (1985).
16. Silva-Bermudez, H. K. & Kzhyshkowska, J. G. Macrophages as a source and target of GDF-15. *Int. J. Mol. Sci.* **25** (13), 7313. <https://doi.org/10.3390/ijms25137313> (2024).
17. Bootcov, M. et al. MIC-1, a novel macrophage inhibitory cytokine, is a divergent member of the TGF- β superfamily. *PNAS* **94** (21), 11514–11519 (1997).
18. Rajendra, S., Apte, D. S., Chen, N. & Ferrara VEGF in signaling and disease: beyond discovery and development. *Cell* **176** (6), 1248–1264. <https://doi.org/10.1016/j.cell.2019.01.021> (2019).
19. Mahdavian, K. et al. Autocrine effect of vascular endothelial growth factor-A is essential for mitochondrial function in brown adipocytes. *Metabolism* **65** (1), 26–35. <https://doi.org/10.1016/j.metabol.2016.01.001> (2016).
20. Villarroja, F., Cereijo, R. & Villarroja, J. Brown adipose tissue as a secretory organ. *Nat. Rev. Endocrinol.* **13** (1), 26–35 (2017).
21. Moon, K. C. et al. Possibility of injecting Adipose-Derived stromal vascular fraction cells to accelerate microcirculation in ischemic diabetic feet: A pilot study. *Int. J. Stem Cells*. **12** (1), 107–113 (2019).
22. Lonardi, R. et al. Autologous micro-fragmented adipose tissue for the treatment of diabetic foot minor amputations: a randomized controlled single-center clinical trial (MiFrAADIF). *Stem Cell. Res. Ther.* **10** (1), 223. <https://doi.org/10.1186/s13287-019-1328-4> (2019).
23. Frühbeck, G. et al. BAT: a new target for human obesity. *Trends Pharmacol. Sci.* **30** (8), 387–396 (2009).
24. Barbatelli, G. et al. The emergence of cold-induced brown adipocytes in mouse white fat depots is determined predominantly by white to brown adipocyte transdifferentiation. *Am. J. Physiol. Endocrinol. Metab.* **298** (6), e1244–1253 (2010).
25. Kahn, C. R., Wang, G. & Lee, K. Y. Altered adipose tissue and adipocyte function in the pathogenesis of metabolic syndrome. *J. Clin. Invest.* **129** (10), 3990–4000 (2019).
26. Gunawardana, S. C. & Piston, D. W. Reversal of type 1 diabetes in mice by brown adipose tissue transplant. *Diabetes* **61** (3), 674–682 (2012).
27. Enerback, S. et al. Mice lacking mitochondrial uncoupling protein are cold-sensitive but not obese. *Nature* **387** (6628), 90–94 (1997).
28. Lowell, B. B. et al. Development of obesity in Transgenic mice after genetic ablation of brown adipose tissue. *Nature* **366** (6457), 740–742 (1993).

29. Bryniarski, A. R., Meyer, G. A. Brown fat promotes muscle growth during regeneration. *J. Orthop. Res.* **37** (8), 1817–1826 (2019).
30. Xu, Z. et al. Single-cell RNA sequencing and lipidomics reveal cell and lipid dynamics of fat infiltration in skeletal muscle. *J. Cachexia Sarcopenia Muscle*. **12** (1), 109–129 (2021).
31. Zhang, H. et al. Preconditioning improves muscle regeneration after ischemia-reperfusion injury. *J. Orthop. Res.* **39** (9), 1889–1897 (2021). We have incorporated the relevant literature into the references.
32. Qiu, L. et al. Browning of human subcutaneous adipose tissue after its transplantation in nude mice. *Plast. Reconstr. Surg.* **172** (2), 392–400 (2018).
33. Zhu, Y. Z. et al. Supplementation with extracellular vesicles derived from adipose-derived stem cells increases fat graft survival and Browning in mice: A cell-free approach to construct beige fat from white fat grafting. *Plast. Reconstr. Surg.* **145** (5), 1183–1195 (2020).
34. Cai, J. et al. Tamoxifen-Prefabricated beige adipose tissue improves fat graft survival in mice. *Plast. Reconstr. Surg.* **141** (4), 930–940 (2018).
35. Forsythe, R. O. & Hinchliffe, R. J. Management of peripheral arterial disease and the diabetic foot. *J. Cardiovasc. Surg. (Torino)*. **55** (2 Suppl 1), 195–206 (2014).
36. Boniakowski, A. E. et al. Macrophage-mediated inflammation in normal and diabetic wound healing. *J. Immunol.* **199** (1), 17–24 (2017).
37. Boniakowski, A. M. et al. SIRT3 regulates macrophage-mediated inflammation in diabetic wound repair. *J. Invest. Dermatol.* **139** (12), 2528–2537 (2019).
38. Falanga, V. Wound healing and its impairment in the diabetic foot. *Lancet* **366** (11), 1736–1743 (2005).
39. Shapouri-Moghaddam, A., Mohammadian, S. & Vazinih Macrophage plasticity, polarization, and function in health and disease. *J. Cell. Physiol.* **233** (9), 6425–6440 (2018).
40. Parisi, L. et al. Macrophage polarization in chronic inflammatory diseases: killers or builders. *J. Immunol. Res.* **2018** (1), 8917804 (2018).
41. Oh, D. S. et al. Activated platelet-rich plasma improves fat graft survival in nude mice: a pilot study. *Dermatol. Surg.* **37** (5), 619–625 (2011).

Acknowledgements

We thank the Center for Basic and Translational Research, the Second Affiliated Hospital Zhejiang University School of Medicine, and School of Pharmaceutical Sciences, Zhejiang Chinese Medical University for their assistance and support in this study. We thank Home for Researchers editorial team (www.home-for-researchers.com) for language editing service.

Author contributions

T.L. and H.J. participated in research design; T.L., A.L., C.L., Y.L. and B.Y. conducted experiments; T.L., H. J. and Q. L. supervised experiments; T.L., A.L., C.L. and L.Q. performed data analysis; T.L. and H.J. wrote the manuscript; T.L., H.J. and Q.L. revised and submitted the manuscript.

Funding

This work was supported by the grants from Zhejiang Province Public Welfare Technology Research Program Experimental Animal Project (GD21C040018), Zhejiang Province Traditional Chinese Medicine Science and Technology Project (2023ZR080), Research Project of Zhejiang Chinese Medical University (2024JKZKTS25).

Declarations

Competing interests

The authors declare no competing interests.

Ethics approval and consent to participate

The protocol of the animal study was reviewed and approved by Laboratory Animal Ethics Committee of Second Affiliated Hospital of Zhejiang University School of Medicine before performance.

Additional information

Supplementary Information The online version contains supplementary material available at <https://doi.org/10.1038/s41598-025-93261-5>.

Correspondence and requests for materials should be addressed to Q.L. or H.J.

Reprints and permissions information is available at www.nature.com/reprints.

Publisher's note Springer Nature remains neutral with regard to jurisdictional claims in published maps and institutional affiliations.

Open Access This article is licensed under a Creative Commons Attribution-NonCommercial-NoDerivatives 4.0 International License, which permits any non-commercial use, sharing, distribution and reproduction in any medium or format, as long as you give appropriate credit to the original author(s) and the source, provide a link to the Creative Commons licence, and indicate if you modified the licensed material. You do not have permission under this licence to share adapted material derived from this article or parts of it. The images or other third party material in this article are included in the article's Creative Commons licence, unless indicated otherwise in a credit line to the material. If material is not included in the article's Creative Commons licence and your intended use is not permitted by statutory regulation or exceeds the permitted use, you will need to obtain permission directly from the copyright holder. To view a copy of this licence, visit <http://creativecommons.org/licenses/by-nc-nd/4.0/>.

© The Author(s) 2025